Unified Modeling Suite for Two-Phase Flow, Convective Boiling and Condensation in Macro-and Micro-Channels

John R. THOME [1,*], Andrea CIONCOLINI [2]

[*] Corresponding author: Tel.: +41 21 693 59 81/82; Fax: +41 21 693 59 60;
[1] Heat and Mass Transfer Laboratory, Ecole Polytechnique Fédérale de Lausanne, Switzerland;
john.thome@epfl.ch
[2] School of Mechanical, Aerospace and Civil Engineering, University of Manchester, UK;
andrea.cioncolini@manchester.ac.uk

Abstract

The present paper focuses on the unified modeling suite for annular flow that the authors have and continue to develop. Annular flow is of fundamental importance to the thermal design and simulation of micro-evaporators and micro-condensers for compact two-phase cooling systems of high heat flux components for the thermal management of computer chips, power electronics, laser diodes and high energy physics particle detectors. First, the unified suite of methods is presented, illustrating in particular the most recent updates. Then, results for convective evaporation of refrigerants in non-circular multi-microchannel configurations for microelectronics cooling are presented and discussed. The annular flow suite includes models to predict the void fraction, the entrained liquid fraction, the wall shear stress and pressure gradient, and a turbulence model for momentum and heat transport inside the annular liquid film. The turbulence model, in particular, allows prediction of the local average liquid film thicknesses and the local heat transfer coefficients during convective evaporation and condensation. The benefit of a unified modeling suite is that all the included prediction methods are consistently formulated and are proven to work well together, and provide a platform for continued advancement based on the other models in the suite.

Keywords: Boiling, Evaporation, Annular Flow, Non-Circular Micro Channel.

1. Introduction

Annular two-phase flow is one of the most important of the two-phase flow regimes because of the large range of industrial applications in which it occurs, such as refrigeration and air conditioning systems, nuclear reactors and chemical processing plants. Annular flow is characterized by a continuous liquid film flowing on the channel wall, surrounding a gas core loaded with entrained liquid droplets that flows in the center of the channel.

Annular flow is of fundamental importance to the thermal design and simulation of micro-evaporators and micro-condensers for compact two-phase cooling systems of high heat flux components for the thermal management of computer chips, power electronics, laser diodes and high energy physics particle detectors. In micro-evaporators, annular flow is even more conspicuous than in macrochannels, since annular flow relegates bubbly and slug flows to only the first 3-10% of the vapor quality range. In convective condensation, annular flow is established almost immediately at the inlet of the channel and persists over most of the condensation process until the condensate floods the channel

The purpose of the present paper is to present the unified modeling suite for annular flow that the authors have and continue to develop, focusing in particular on the prediction of the pressure drop and the heat transfer coefficient during convective evaporation in non-circular multi-microchannels that are typical of microscale heat sinks. Presently, the unified annular flow

modeling suite includes methods to predict the entrained liquid fraction, the void fraction, the walls shear stress, the frictional and total pressure gradients, and a turbulence model for momentum and heat transport inside the annular liquid film that allows *one method* for the prediction of the local average liquid film thickness and the local heat transfer coefficient during *both* convective evaporation and condensation (Cioncolini et al., 2009a,b; Cioncolini and Thome, 2011; 2012a,b,c). The practical advantage of a unified modeling suite is that all the included prediction methods are consistently formulated and are proven to work well together. The heat transfer methods have been adapted to non-circular (rectangular and square) microchannels as well as the microchannels in a multi-port aluminum tube, without changing of the underlying equations but just stretching of the liquid film to the non-circular channel cross section.

2. Overview of the Annular Flow Models

In the flow boiling literature, most methods segregate the nucleate boiling and convective boiling contributions and then develop individual methods for each, and then use some form of superposition method to add them together to obtain their combined influence on the local flow boiling heat transfer coefficient. As such, Cioncolini and Thome (2011) focused on convective evaporation in annular flow in the absence of wall nucleation and proposed a new algebraic turbulence model for the transport of linear momentum and heat through the annular liquid film. Algebraic models are simple turbulence models that rely on the Boussinesq assumption and consider the turbulent shear stress to be proportional to the symmetric part of the mean velocity gradient and the turbulent heat flux to be proportional to the mean temperature gradient. The constants of proportionality are flow-dependent and are expressed with empirically derived algebraic relations that involve the length scale of the mean flow. In contrast with single-phase wall-bounded flow theory, normally extrapolated to two-phase flows in most existing studies, the authors assumed that the flow in the shear-driven annular liquid film is mostly affected by the interaction of the liquid film with the shearing gas-entrained droplet core flow. In other words, the liquid film was assumed to behave as a fluid-bounded flow, such as a jet or a wake, with a negligible influence of the bounding channel wall. Since the characteristic length scale of jets and wakes is normally assumed to be proportional to their width, the characteristic length scale of the liquid film was thus assumed to be proportional to its average thickness, instead of the distance from the channel wall used in single-phase wall-bounded turbulent flows.

The heat transfer equation proposed by the authors for convective evaporation in annular flow reads as follows:

$$Nu = \frac{ht}{k_l} = 0.0776\, t^{+0.90} Pr_l^{0.52} \qquad 10 \le t^+ \le 800;\ 0.86 \le Pr_l \le 6.1 \tag{1}$$

where h is the convective evaporation heat transfer coefficient, k_l is the liquid thermal conductivity, Nu is a Nusselt number based on the average liquid film thickness t, Pr_l is the liquid Prandtl number and t^+ is the dimensionless liquid film thickness expressed in wall coordinates and defined as:

$$t^+ = \frac{t}{y^*} = \frac{\rho_l V^* t}{\mu_l};\ y^* = \frac{\mu_l}{\rho_l V^*};\ V^* = \sqrt{\frac{\tau_w}{\rho_l}} \tag{2}$$

where ρ_l and μ_l are the liquid density and viscosity, y^* and V^* are the length and velocity wall scales and τ_w is the wall shear stress. According to the authors, the dimensionless liquid film thickness is empirically predicted as follows:

$$t^+ = \max\left(\sqrt{\frac{Re_{lf}}{2}},\ 0.0165\, Re_{lf} \right) \tag{3}$$

where the liquid film Reynolds number Re_{lf} is defined as:

$$Re_{lf} = (1-e)(1-x)\frac{Gd}{\mu_l} \tag{4}$$

where e is the entrained liquid fraction, x the vapor quality, G the total mass flux and d the tube diameter. As can be seen, Eq. (1) is formally analogous to a Dittus-Boelter like heat transfer equation, since the dimensionless liquid film thickness t^+ can be interpreted as a Reynolds number for the liquid film with the velocity wall scale V^* as characteristic velocity and the average liquid film thickness t as the characteristic dimension.

The wall shear stress τ_w that is required as input in Eq. (2) to calculate the velocity wall scale V^* is predicted according to Cioncolini et al. (2009) as follows:

$$f_{tp} = \frac{2\tau_w}{\rho_c V_c^2} = 0.172\, We_c^{-0.372} \quad for\ Bo \geq 4 \quad (macrochannels) \tag{5}$$

$$f_{tp} = \frac{2\tau_w}{\rho_c V_c^2} = 0.0196\, We_c^{-0.372} Re_{lf}^{0.318} \quad for\ Bo \leq 4 \quad (microchannels) \tag{6}$$

where f_{tp} is the two-phase Fanning friction factor. The droplet-laden core flow density ρ_c and average core velocity V_c are calculated neglecting the slip between the carrier gas phase and the entrained liquid droplets as follows:

$$\rho_c = \frac{x + e\,(1-x)}{\dfrac{x}{\rho_g} + \dfrac{e\,(1-x)}{\rho_l}};\ V_c = \frac{J_g}{\varepsilon};\ J_g = \frac{x\,G}{\rho_g} \tag{7}$$

where J_g is the vapor superficial velocity and ε the cross sectional void fraction. The core flow Weber number We_c and the Bond number Bo are defined as:

$$We_c = \frac{\rho_c J_g^2 d}{\sigma} \tag{8}$$

$$Bo = \frac{g\left(\rho_l - \rho_g\right)d^2}{\sigma} \tag{9}$$

where σ is the surface tension and g the acceleration of gravity.

The entrained liquid fraction e required as input into Eqs. (4) and (7) is predicted according to Cioncolini and Thome (2012b) as follows:

$$e = \left(1 + 279.6\, We_c^{-0.8395}\right)^{-2.209} \quad for \quad 10^1 < We_c < 10^5 \tag{10}$$

The void fraction ε required as input in Eq. (7) is predicted according to Cioncolini and Thome (2012a) as follows:

$$\varepsilon = \frac{h\,x^n}{1 + (h-1)\,x^n} \quad 0 < x < 1;\ 10^{-3} < \rho_g \rho_l^{-1} < 1;\ 0.7 < \varepsilon < 1 \tag{11}$$

where the parameters h and n are:

$$h = -2.129 + 3.129\,(\rho_g \rho_l^{-1})^{-0.2186}$$
$$n = 0.3487 + 0.6513\,(\rho_g \rho_l^{-1})^{0.5150} \tag{12}$$

Using the two-phase Fanning friction factor given by either Eq. (5) or Eq. (6) together with Eq. (8) for the core Weber number, the two-phase frictional pressure gradient is calculated as follows:

$$\left(\frac{dP}{dz}\right)_{fr} = \frac{4\tau_w}{d} = \frac{2 f_{tp}}{d}\rho_c V_c^2 \tag{13}$$

For inclined flow, the gravitational pressure gradient is calculated as:

$$\left(\frac{dP}{dz}\right)_{gr} = \left[\rho_l(1-\varepsilon) + \rho_g \varepsilon\right] g \sin(\theta) \tag{14}$$

where θ is the channel inclination with respect to the horizontal (θ = 0 for horizontal flow), while the acceleration pressure gradient is calculated as follows:

$$\left(\frac{dP}{dz}\right)_{acc} = G^2 \frac{d}{dz}\left\{\begin{array}{l}\dfrac{(1-e)^2(1-x)^2 x}{(1-\varepsilon)\,x\,\rho_l} + \\ \dfrac{e\,x\,(1-x)}{\varepsilon\,\rho_g} + \dfrac{x^2}{\varepsilon\,\rho_g}\end{array}\right\} \tag{15}$$

The unified annular flow modeling suite is currently based on a large experimental databank collected from 99 literature studies that contains 11498 data points, and additional work is being performed to expand the underlying database and further improve the annular flow models. Selected results for convective evaporation in non-circular multi-microchannels are presented below.

3. Results for Non-Circular Microchannels

Based on available data, the annular flow models for the wall shear stress, the entrained liquid fraction and the void fraction previously discussed can be extrapolated to non-circular channels using the hydraulic diameter d_h ($d_h = 4\ A_{flow}\ P_{wet}^{-1}$, where A_{flow} is the flow area and P_{wet} the wetted perimeter) in place of the tube diameter. For what concerns the convective evaporation heat transfer model, Costa-Patry et al. (2011a,b; 2012) proposed a simple adaptation of the Cioncolini and Thome (2011) annular flow method for evaporation for circular channels to non-circular shapes, i.e. high aspect ratio rectangular fins in silicon and copper in particular. Vakili-Farahani et al. (2012) and Szczukiewicz et al. (2013) also found that this adaption works well for non-circular microchannels for an aluminum multi-port tube test section and for a multi-microchannel test section with square channels of only 100 by 100 microns, respectively. These adaptions and comparisons will be discussed below.

In a circular channel, the original method balances the forces in the channel to calculate a radial film thickness, while in a non-circular (rectangular for instance) channel this film must be redistributed to the actual channel perimeter, keeping the same area proportion between the shapes and to conserve the liquid cross-sectional area proportions. To do this, the equivalent diameter d_{eq} is used, which is the diameter of an equivalent circular channel with the same cross-sectional area as the non-circular one…*a hydraulic diameter in fact has no apparent physical meaning in an annular flow with its liquid film*. As a consequence of this adaptation, the average film thickness in the non-circular channel is less than the circular one since the liquid film of the equivalent diameter's perimeter is stretched to the perimeter of the actual channel to maintain the same cross-sectional area of the liquid within the channel…essentially, since the thermal resistance across the film determines the annular flow heat transfer coefficient, this is a simple correction to implement while ignoring capillary forces in any corners. In practice, the liquid film thickness is first calculated for the equivalent circular pipe and then the cross-sectional area A_{lf} taken by the circular film is calculated as:

$$A_{lf} = \frac{\pi}{4}\left[d_{eq}^2 - (d_{eq} - 2\delta)^2\right] \qquad (16)$$

Since the liquid film must occupy the same area in the non-circular shape as in the circular channel, the liquid film thickness in the non-circular channel is found by dividing the liquid film cross-sectional area by the non-circular channel perimeter ($\delta = A_{lf}\ P_{wet}^{-1}$). The Nusselt number calculated by the method is finally transformed into a heat transfer coefficient by dividing it by this non-circular channel liquid film thickness.

In contrast, for predicting two-phase frictional pressure drops in non-circular channels, the unified annular flow suite is applied using directly the hydraulic diameter in place of the circular diameter without further modification. In this case, the frictional pressure gradient is dependent on the interfacial shear between the vapor core and the annular liquid film, but not on the liquid film thickness, in Eqs. (5) and (6). Hence, both heat transfer and two-phase frictional pressure drops were adapted to non-circular flow channels without adding or changing any numerical values in the annular flow suite's methods.

In order to handle the other relevant flow regimes in microscale channels, notably isolated bubble flow and elongated bubble flow, these annular flow models have been recently extended (Costa-Patry et al., 2011a,b 2012; Vakili-Farahani et al., 2012 and Szczukiewicz et al., 2013) by combining them with the Lockhart and Martinelli (1949) method to predict the pressure gradient, and with the Cooper (1984) nucleate pool boiling correlation and the three-zone convective heat transfer model (Thome et al., 2004) to predict the heat transfer coefficient in the isolated bubble flow regime and in the elongated bubble flow regime, respectively.

The three-zone heat transfer model, in particular, treats evaporation of elongated

bubbles in microchannels as a cyclic passage of: a liquid slug, an evaporating elongated bubble, and a vapor slug, which is assumed to appear when the liquid film thickness near the bubble tail reaches the same value as the surface roughness of the channel. The transition from isolated bubble flow to elongated bubble flow and from elongated bubble flow to annular flow is predicted according to the microscale flow map of Ong and Thome (2011).

Costa-Patry et al. (2011a,b; 2012) investigated two-phase flow evaporation of refrigerants R245fa and R236fa flowing in 135 high aspect ratio silicon multi-microchannels, as shown in Fig. 1.

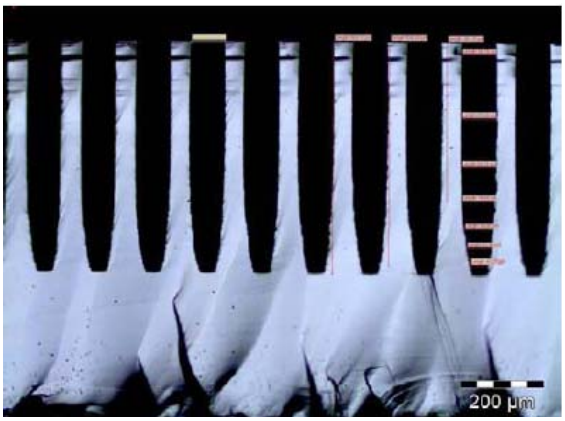

Figure 1. Silicon multi-microchannel test section used by Costa-Patry et al. (2011a,b; 2012): cut view of the evaporator channels [135 parallel channels, height: 560 µm; width: 85 µm; aspect ratio: 6.56; hydraulic diameter: 136 µm; fin thickness: 47 µm; channels length: 12.7 mm].

The channels were 85 μm-wide, 560 μm-high, aspect ratio of 6.56, hydraulic diameter of 136 μm, 12.7 mm-long, and separated by 47 μm-wide fins. The multi-microchannels were electrically heated with 35 local heaters that could be operated independently, thus allowing tests to be performed with both uniform and non-uniform heating to more closely reproduce the heat load of actual microchips. Measurements carried out under uniform heat flux conditions for the pressure drop and the heat transfer coefficient are compared with the predictions of the annular flow models extended to non-circular microchannels in Figs. 2 and 3. As can be seen, the agreement between measured data and predictions is quite satisfactory.

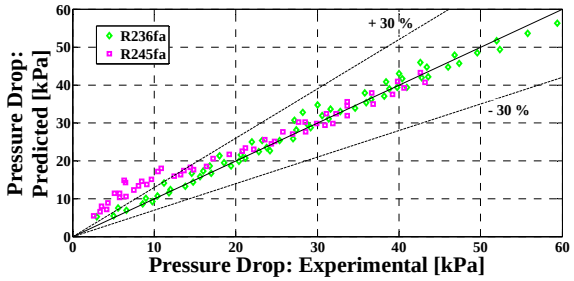

Figure 2. Boiling two-phase flow results of Costa-Patry *et al.* (2011a,b): predictions versus measurements for the pressure drop under uniform heat flux conditions [fluids: R236fa and R245fa; saturation temperature: 303 K].

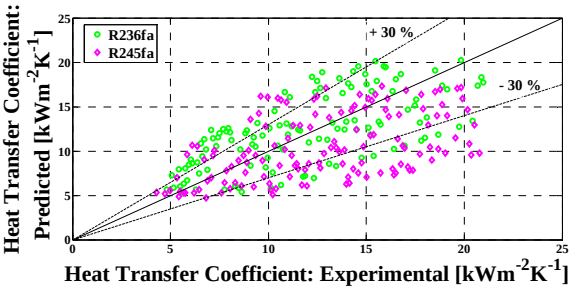

Figure 3. Boiling two-phase flow results of Costa-Patry et al. (2011a,b): predictions versus measurements for the heat transfer coefficient under uniform heat flux conditions [fluids: R236fa and R245fa; saturation temperature: 303 K].

Heat transfer coefficients measured under non-uniform heat flux conditions are compared with the annular flow models predictions in Fig. 4.

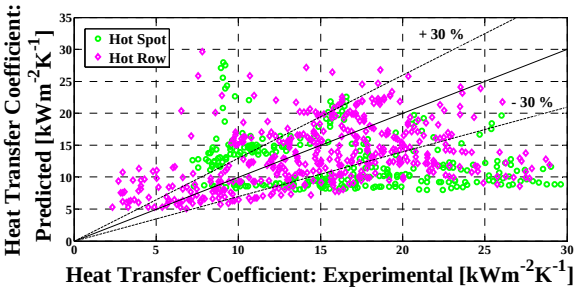

Figure 4. Boiling two-phase flow results of Costa-Patry et al. (2012): predictions versus measurements for the heat transfer coefficient under non-uniform heat flux conditions [fluid: R245fa; saturation temperature: 303 K].

In particular, both hot-spot and hot-row heat flux profiles have been tested, as shown

in Fig. 5, and implementing a heat spreading data reduction procedure to obtain the local heat transfer coefficients.

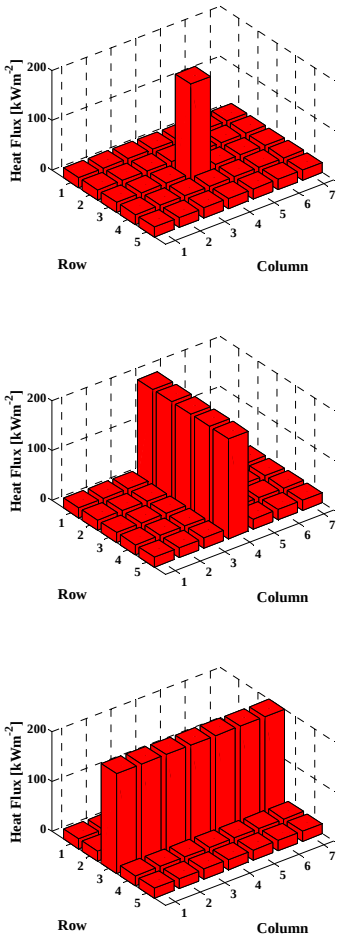

Figure 5. Non-uniform heat flux profiles tested by Costa-Patry et al. (2012): hot-spot (top), hot-row aligned with the flow (middle) and hot-row perpendicular to the flow (bottom).

Although less accurate than with uniform heating, the annular flow models extended to non-circular microchannels predict the non-uniform heating data with a mean average error of less than 30%, which is quite good when taking into account the larger experimental uncertainty found in non-uniform heat flux situations.

Vakili-Farahani et al. (2012) carried out two-phase flow evaporation experiments with refrigerants R245fa and R1234ze(E) in the flat aluminum extruded multi-port tube shown in Fig. 6. The multiport tube was composed of 7 parallel rectangular channels 1.1 mm-wide, 2.1 mm-high, aspect ratio of 1.91, equivalent diameter of 1.7 mm and 280 mm-long. The channels were fluid heated with a hot water jacket on both sides. The system tested was a prototype cooling element for a two-phase thermosyphon electronics cooling system, which has since been commercialized by ABB for 15 MVA transformers with up to 112 kW of cooling load. Measurements of their heat transfer coefficients are compared with the predictions of the annular flow model suite extended to non-circular microchannels in Fig. 7. As can be seen, the agreement between measured data and predictions is quite satisfactory…the over-predictions at higher values are thought to come from test conditions that have surpassed the onset of partial dryout, i.e. the center faces of the channel walls may become dry during evaporation.

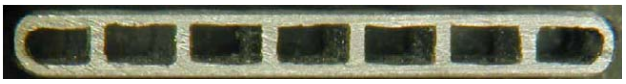

Figure 6. Flat aluminum extruded multiport tube used by Vakili-Farahani et al. (2012) [7 parallel rectangular channels, height: 1.1 mm; width: 2.1 mm; aspect ratio: 1.91; hydraulic diameter: 1.4 mm; equivalent diameter: 1.7 mm; channel length: 280 mm].

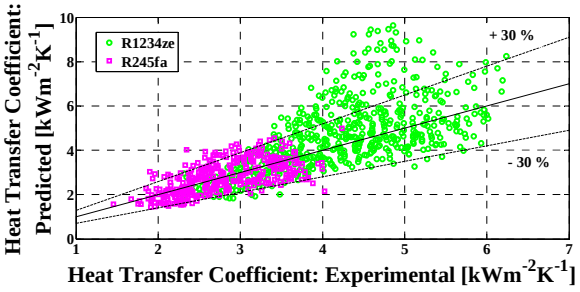

Figure 7. Boiling two-phase flow results of Vakili-Farahani et al. (2012): predictions versus measurements for the heat transfer coefficient [fluids: R245fa and R1234ze(E); saturation temperature: 303-343 K]

Szczukiewicz et al. (2013) investigated two-phase flow evaporation of refrigerants R245fa, R236fa and R1234ze(E) flowing in 67 square cross section, silicon multi-microchannels, as shown in Fig. 8. The channels were 100x100 μm size, aspect ratio of 1.0, hydraulic diameter of 100 μm, 10.0

mm-long, and separated by 50 μm-wide fins. Electrical heating with uniform heat flux was used in the tests.

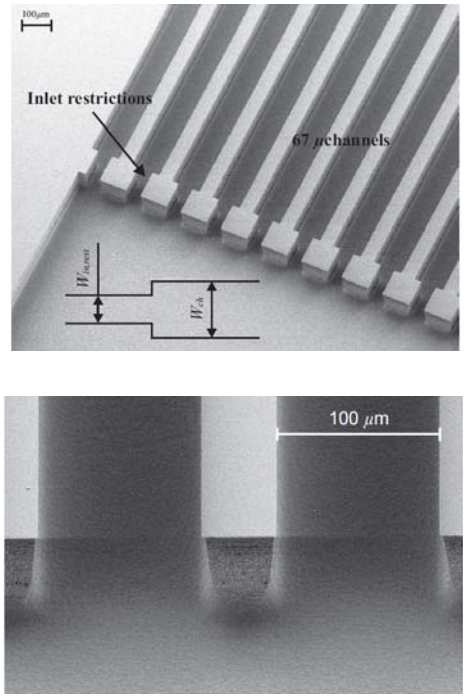

Figure 8. Silicon multi-microchannel test section used by Szczukiewicz et al. (2013): detail of the evaporator channels with inlet restrictions to stabilize the flow [67 parallel square channels, height: 100 µm; width: 100 µm; aspect ratio: 1.0; hydraulic diameter: 100 µm; fin thickness: 50 µm; channels length: 10.0 mm].

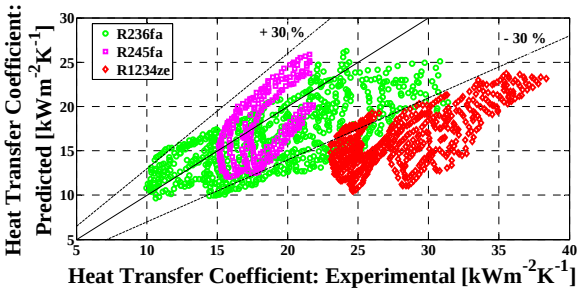

Figure 9. Boiling two-phase flow results of Szczukiewicz et al. (2013): predictions versus measurements for the heat transfer coefficient under uniform heat flux conditions [fluids: R236fa, R245fa and R1234ze(E); saturation temperature: 305 K].

The system tested was one layer of a future three-dimensional integrated circuit stacked architecture with interlayer cooling, and was part of the *CMOSAIC - 3D Stacked Architectures with Interlayer Cooling* project whose aim was to provide two-phase cooling to a high-performance, three-dimensional stacked computer chip that will eventually compress almost 1012 nm-sized functional units into a volume of 1 cm^3 with a 10 to 100 fold higher connectivity than otherwise possible (Sabry et al., 2011).

Measurements carried out under uniform heat flux conditions for the heat transfer coefficient are compared with the predictions of the annular flow models extended to non-circular microchannels in Fig. 9. As can be seen, the agreement between measured data and predictions is quite satisfactory for R236fa and R245fa, while the R1234ze(E) data are somewhat underpredicted. According to the authors, this might be due to a larger flashing effect for R1234ze(E), the highest pressure refrigerant tested, or due to the micro-orifice entrance that makes a jet-like flow down the beginning of the channel.

4. Conclusions

The unified modeling suite for annular two-phase flow that the authors have and continue to develop was presented, illustrating in particular its application to non-circular microchannels. The convective heat transfer model was then compared with selected measurements, obtained by the LTCM lab for refrigerant convective evaporation in non-circular multi-microchannels configurations for electronics cooling. Satisfactory agreement was found between data and predictions. This unified modeling suite provides a robust set of methods that are so far proven to work well together in a situation where the various flow parameters are interrelated and provides a basis for future additional developments.

5. References

Cioncolini, A., Thome, J.R., Lombardi, C., 2009a, Algebraic turbulence modeling in adiabatic gas-liquid annular two-phase flow, Int. J. Multiphase *Flow* 35, 580-596.

Cioncolini, A., Thome, J.R., Lombardi, C., 2009b. Unified macro-to-microscale method to predict two-phase frictional pressure drops of annular flows. Int. J. Multiphase Flow 35, 1138-1148.

Cioncolini, A., Thome, J.R., 2011. Algebraic turbulence modeling in adiabatic and evaporating annular two-phase flow. Int. J. Heat Fluid Flow 32, 805-817.

Cioncolini, A., Thome, J.R., 2012a. Void fraction prediction in annular two-phase flow. Int. J. Multiphase Flow 43, 72-84.

Cioncolini, A., Thome, J.R., 2012b. Entrained liquid fraction prediction in adiabatic and evaporating annular two-phase flow. Nucl. Eng. Des. 243, 200-213.

Cioncolini, A., Thome, J.R., 2012c, Algebraic turbulence modeling in condensing annular two-phase flow: preliminary results. ECI 8th International Conference on Boiling and Condensation Heat Transfer, Lausanne, Switzerland, 3-7 June 2012, paper number 1536.

Cooper, M.G., 1984. Heat flow rates in saturated nucleate pool boiling - a wide ranging examination using reduced properties, Adv. Heat Transfer 16, 157-239.

Costa-Patry, E., Olivier, J., Nichita, B., Michel, B., Thome, J.R., 2011a. Two-phase flow of refrigerants in 85μm-wide multi-microchannels, Part I: pressure drop. Int. J. Heat Fluid Flow 32, 451-463.

Costa-Patry E., Olivier, J., Michel, B., Thome, J.R., 2011b. Two-phase flow of refrigerant in 85 μm-wide multi-microchannels: Part II: heat transfer with 35 local heaters. Int. J. Heat Fluid Flow 32, 464–476.

Costa-Patry, E., Nebuloni, S., Olivier, J., Thome, J.R., 2012. On-chip two-phase cooling with refrigerant 85 μm-wide multi-microchannel evaporator under hot-spot conditions. IEEE Trans. Compon. Packag. Manuf. Technol. 2, 311-320.

Lockhart, R.W., Martinelli, R.C., 1949. Proposed correlation of data for isothermal two-phase, two-component flow in pipes. Chem. Eng. Prog. 45, 39–48.

Ong, C.L., Thome, J.R., 2011. Macro-to-microchannel transition in two-phase flow: Part I – Two phase flow patterns and film thickness measurements. Exp. Thermal Fluid Science 35, 37–47.

Sabry, M. M., Sridhar, A., Atienza, D., Temiz, Y., Leblebici, Y., Szczukiewicz, S., Borhani, N., Thome, J. R., Brunschwiler, T., Michel, B., 2011. Towards thermally-aware design of 3D MPSoCs with inter-tier cooling. In Design, Automation and Test in Europe.

Szczukiewicz, S., Borhani, N., Thome, J.R., 2013. Fine-resolution two-phase flow heat transfer coefficient measurements of refrigerants in multi-microchannel evaporators, Int. J. Heat Mass Transfer 67, 913-929.

Thome, J.R., Dupont, V., Jacobi, A.M., 2004. Heat transfer model for evaporation in microchannels. Part I: presentation of the model. Int. J. Heat Mass Transfer 47, 3387–3401.

Vakili-Farahani, F., Agostini, B., Thome, J.R., 2012. Experimental study on flow boiling heat transfer of multiport tubes with R245fa and R1234ze(E). ECI 8th International Conference on Boiling and Condensation Heat Transfer, Lausanne, Switzerland, 3-7 June 2012, paper number 1480.